Recognition of Palmprints using Eigenpalm

Ajay Kumar, Helen C. Shen
Department of Comp uter Science
Hong Kong University of Science and Technology
Clear Water Bay, Hong Kong
Email: {*ajaykr, helens*}*@cs.ust.hk*

Abstract

This paper presents a new method for personal recognition using palmprints. This method uses, inkless, normalized palmprint images to generate eigenpalms. Every palmprint image is thus characterized by a feature vector, consisting of weights from eigenpalm images. The performance of proposed method using two measures i.e., minimum Euclidean distance and maximum similarity measure, is evaluated. The low-resolution images of 100 dpi, which dominantly capture the palmprint creases, have been used in the experiments. The experimental results show that this method achieves high recognition rate when the similarity criterion is used to recognize 300 inkless palmprint test images.

1. Introduction

Biometrics systems that can be used for personal recognition are in increasing demand. Much of the prior work on personal recognition has been focused on biometrics features such as face and fingerprint. Palmprint refers to the pattern of skin on the surface of the palm and is unique for every individual. As compared to fingerprint, the palmprint have large number of creases and has been found appropriate as a feature for identification. The utility of palmprint images, for personal identification, using wavelets [1], Fourier Features [2], and local texture features [3]-[5] have been presented in the literature.

The information content of palmprint image also consists of certain local and global features that can be used for identification. This information can be extracted by registering the variations in an ensamble of palmprint images, independent of any judgment of palmprint lines or creases. This paper investigates such an unsupervised statistical approach for the palmprint recognition.

The usefulness of inkless palmprint images has been investigated in [1]-[4]. Therefore the performance of the proposed approach has been evaluated on real inkless palmprint images. Any commercial development of an automated palmprint based identification system would require automated extraction of region of interest *i.e.* palmprint area, while ignoring fingers, wrist, and background (if any). This paper also presents an elegant and simple method for the automated selection of palmprint area from the composite hand image.

2. Methodology

Each of the acquired hand images (figure 1) are first binarized using gray-level thresholding. The magnitude of appropriate thresholding limit is computed automatically using Otsu's method [6]. The binarized image is subjected to the morphological erosion to compute the region of interest. In our experiments we have used 290 × 290 pixels palmprint images. Therefore a square structuring element (*SE*) of size 145 × 145 pixels was found appropriate and used. The palmprint area in composite hand images is not perfectly square or aligned vertically. Therefore, depending on the structure and size of selected *SE*, after every erosion operation a residue of the binarized image is expected. The center of this residual image *i.e.* the center of rectangle that can enclose the residue is determined. This center coordinates are used to extract the squares palmprint region, of fixed size, from the composite hand image, as shown in figure 3. The block diagram of the recognition process is shown in figure 2.

2.1. Normalization

Every N × N pixel palmprint image can be represented by a vector Ω of $1 \times N^2$ dimension using row ordering. Let the training set of palmprint images be represented by $\{\Omega | j = 1,..., K\}$. Each of these palmprint images are normalized to have zero mean and unity variance. This involves the computation of mean and variance of the training palmprint images.

$$w = \frac{1}{K}\sum_{j=1}^{K}\Omega_i \qquad y^2 = \frac{1}{K}\sum_{j=1}^{K}(\Omega_j - w)^2 \tag{1}$$

The above two images are used to compute the normalized set of training images $\Phi = [\Theta_1, \Theta_2, ..., \Theta_K]$ where

$$\Theta_j = \frac{\Omega_j - w}{y}, \qquad j = 1, 2, . . , K \tag{2}$$

The sensor noise and palm pressure difference results in palmprint images of varying brightness and contrast. The normalization (2) is used to remove these offsets in the image acquisition. These normalized images or vectors are used to compute eigenpalms, as described in the following section.

2.2. Eigenpalms

The normalized set of training vectors are subjected to principal component analysis. The principal component

analysis generates a set of orthonormal vectors that can optimally represent the information in the dataset. Each of these orthonormal vectors (or eigenvectors) are designated as eigenpalms, similar to as eigenfaces in [7]. The covariance matrix of normalized vectors Θ_j can be obtained as follows.

$$C = \frac{1}{K}\sum_{j=1}^{K}\Phi\Phi^T \quad (3)$$

The computation of eigenvector of $N^2 \times N^2$ covariance matrix **C** is cumbersome due to the memory and computational constraints. Therefore the simplified method suggested in [6 is adopted. Thus the eigenvectors $Z[v_1, v_2, ..., v_K]$ of the $M \times M$ matrix Γ are first computed.

$$\Gamma = \Phi^T\Phi \quad (4)$$

The eigenvectors of covariance matrix **C**, say $u_j (j = 1,2,..., K)$, are computed from the product of Θ_j and v_j.

$[u_1, u_2, ..., u_K] = [\Theta_1, \Theta_2, ..., \Theta_K][v_1, v_2, ..., v_K]$, or

$$U = \Phi Z \quad (5)$$

Each of the basis vectors u_j in (5) is the ordered principal components of covariance matrix **C**. These $1 \times N^2$ dimension vectors can be lexicographically reordered to obtain $N \times N$ pixel images designated as *eigenpalm*. Each of the eigenpalms look like ghostly palm image (figure 6), in which each pixel accounts for deviation of the pixel value from the corresponding mean palm value in the training set. These eigenpalms are used to describe every palmprint image using a feature vector. This feature vector in essence is a weighted sum of eigenpalm features.

Each of the K eigenpalms are used to compute characteristic features for each of the training palmprint images. This is achieved by computing a set of projection coefficients for each of the training palmprint images, on a set of K' eigenpalm vectors. Thus the features vector $\omega_j^T = [x_1, x_2, ..., x_{K'}]$ for j^{th} training palmprint image is obtained as follows:

$$x_i = u_i^T\Theta_j \quad i = 1,2,..., K', \qquad j = 1,2,..., K, \qquad K' \le K \quad (6)$$

The (i) set of feature vectors ω_j from every users, (ii) set of eigenpalms u_j, and (iii) with mean and variance palm vectors *i.e.* m and v, are stored during the training phase. These stored vectors are used during the recognition of an unknown user.

3. Recognition

The palmprint image of an unknown user, to be recognized, is first normalized. As shown in figure 2, the mean and variance palmprint training images obtained from the training phase are used for the normalization (2). This normalized vector is then projected into the subspace spanned by K' eigenpalms. Thus the characteristic features of an unknown user are obtained using (6), which form the feature vector $y^T = [y_1, y_2, ..., y_{K'}]$. This feature vector y is compared with the each of the feature vectors of users *i.e.* ω_j. The best possible match is assigned to unknown user. Two measures for matching between feature vector y and ω_j are considered; (i) maximum similarity [3] between feature vectors, and (ii) minimum Euclidean distance [7] between feature vectors. These two measures in (i) and (ii) are represented as $S_{\max}$ and $D_{\min}$ respectively.

$$S_{\max} = \max_j\left\{\frac{\sum_i y_j}{\sqrt{\sum_i y_j \sum_i \omega_j}}\right\} \quad (7)$$

$$D_{\min} = \min_j\left\{\|y - \omega_j\|_2\right\} \quad (8)$$

The similarity measure in (7) computes the normalized correlation between vectors y and ω_j, for each of the trained class *j*. The class label *j* is assigned to the unknown user *i.e.* y, using the best available match from (7) or (8).

4. Experiments

The inkless palmprint images obtained from the HP-ScanJet ADF scanner are used in the experiments. The image database consists of 300 images (100 dpi, 290×290 pixel) from the 15 persons (users), 10 each from the right and left palm. One palmprint image from each of the users, from each of the right and left palms, was used for the training. The training palmprint image from left palm, for each of the users, is shown in figure 4. Three different sets of experiments were performed; recognition using (i) left palmprint images, (ii) right palmprint images, and (iii) when the right and left palmprint images from a user are assumed to be belonging to the two different users.

5. Results

The experimental results for recognition using palmprint images were excellent. Figure 5 shows the mean and variance of the training palmprint images for left palm. The first eight eigenpalms obtained during the training of left palmprint images, in the decreasing order of variance, are shown in figure 6. Table 1 shows the maximum recognition rate obtained for each of the three experiments, as described in previous section. The recognition rates in table 1 were obtained when the all the available eigenpalms were used. It can be observed from this table

that the recognition rates obtained from the case when similarity measure $S_{\max}$ is used outweigh the case when Euclidean distance criterion $D_{\min}$ is employed. The variation of error rate with the eigennumber (number of eigenpalms) is displayed in figure 7. This figure also shows comparative error rates using two different matching criterion. The variation of error rates in the palmprint recognition, when the left and right palms are assumed to be belonging to different class *i.e*. 30 class experiment, can be observed in figure 8. This figure also shows that the achieved performance of the matching criterion based on similarity measure (7) is better than the measure in (8).

Two conclusions can be drawn from the results obtained in figure 7 and 8. Firstly, the performance of matching criterion using similarity measure in is superior then the measure based on minimum Euclidean distance, for all the three different sets of experiments. Secondly, the performance of recognition system generally increases with the increase in eigennumbers *i.e*. K' or number of eigenpalms. However this effect is true for a small increase in K' and the performance is insensitive to the large increase in K' (say $K' > 20$ in figure 8). This observation is similar to the performance observed in [7] for the face recognition. Results in table 1 suggests that the achieved performance of recognition using left palm is better than those using right palms. Table 1 also shows the decrease in recognition rate when the palms of the same person were assumed to be belonging to two different users. This could be due to the fact that there exists [9] a lot of similarity (*e.g*. in the principal lines) in both palms of an individual.

6. Conclusion

This paper has presented a new method for personal recognition using eigenpalms. The proposed method uses similarity measure for the feature matching and has been shown to perform better than Euclidean distance used in [7] for face recognition. The experimental results demonstrate the usefulness of palmprint features, even in the two different hands of an individual, for personal recognition. The proposed method can be used to enhance the level of confidence in existing biometrics-based recognition system, or can be used as substitute for fingerprint-based recognition system when it is not feasible to acquire fingerprints from wide range of users *i.e*. users with dry skin, manual laborers, elderly, handicapped, *etc*.. The suggested method of palmprint recognition is simple, fast and tailored for its practical usage. The performance of this method is based on high degree of correlation between the pixel intensities in the training and test images. This correlation is ensured by the palm alignment during imaging and by extensive preprocessing to normalize the images. The accuracy of our results in section 5 may be limited to the size of employed (available) database and therefore an increase in the size of image database, for performance analysis, is desirable.

7. References

[1] A. Kumar and H. C. Shen, "Recognition of palmprints using wavelet-based features," *Proc. Intl. Conf. Sys., Cybern.*, SCI-2002, Orlando, Florida, Jul. 2002.

[2] W. Li, D. Zhang, and Z. Xu, "Palmprint identification by Fourier transform," *Int. J. Patt. Recognit. Art. Intell*., vol. 16, no. 4, pp. 417-432, 2002.

[3] C.-C. Han, H.-L. Cheng, C.-L. Lin and K.-C. Fan, "Personal authentication using palm-print features," *Pattern Recognit*., vol. 36, pp. 371-381, 2003.

[4] A. Kumar, D. C. M. Wong, H. C. Shen, and A. K. Jain, "Personal verification using palmprint and hand geometry biometric, to appear in *Proc. AVBPA 2003*, Guildford (UK), June 2003.

[5] J. You, W. Li, and D. Zhang, "Hierarchical palmprint identification via multiple feature extraction," *Pattern Recognit*., vol. 35, pp. 847-859, 2002.

[6] N. Otsu, "A threshold selection method from gray-scale histogram," *IEEE Trans. Syst., Man, Cybern*., vol. 8, pp. 62-66, 1978.

[7] M. A. Turk and A. P. Pentland, "Eigenfaces for Recognition," *J. Cognitive Neuroscience*, vol. 3, no. 1, pp. 71-76, 1991.

[8] D.-M Tsai and C.-H. Chiang, "Rotation-invariant pattern matching using wavelet decomposition," *Pattern Recognit. Lett*., vol. 23, pp. 191-201, Jan. 2002.

[9] J. Chen, C. Zhang, and G. Rong, "Palmprint recognition using crease," *Proc. Intl. Conf. Image Process*., pp. 234-237, Oct. 2001.

Table 1: Maximum recognition rate from the experiments.

Recognition Rate (%)	Similarity Measure	Euclidean Distance
Left palm (15 classes)	99.33	96.67
Right palm (15 classes)	98.67	95.33
Both palms (30 classes)	98.67	93.67

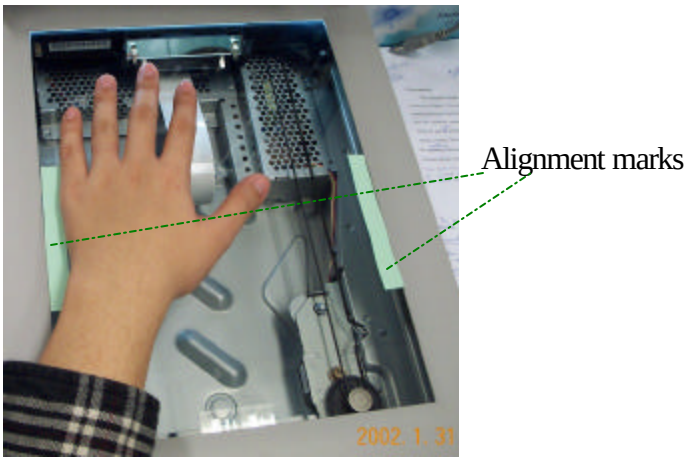

Figure 1: Acquisition of inkless palmprint images from the users.

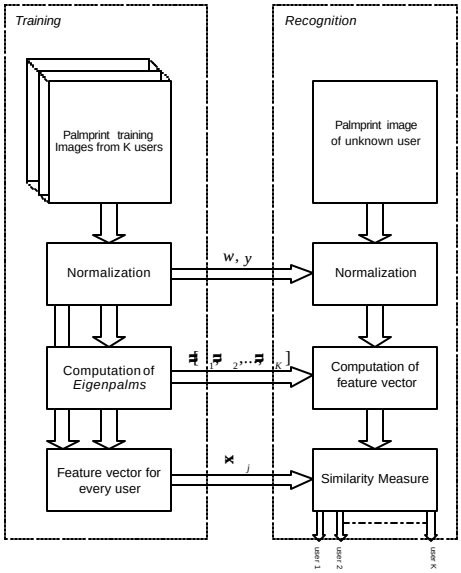

Figure 2: Block diagram for the *Eigenpalm* based palmprint recognition.

(a) (b) (c) (d) (e)

Figure 3: (a) Acquired image from the image sensor, (b) Image after thresholding using Otsu's limit, (c) Image after morphological erosion, (d) palmprint *i.e*. square generated from the center of limits of observed region in (c), (e) Extracted palmprint.

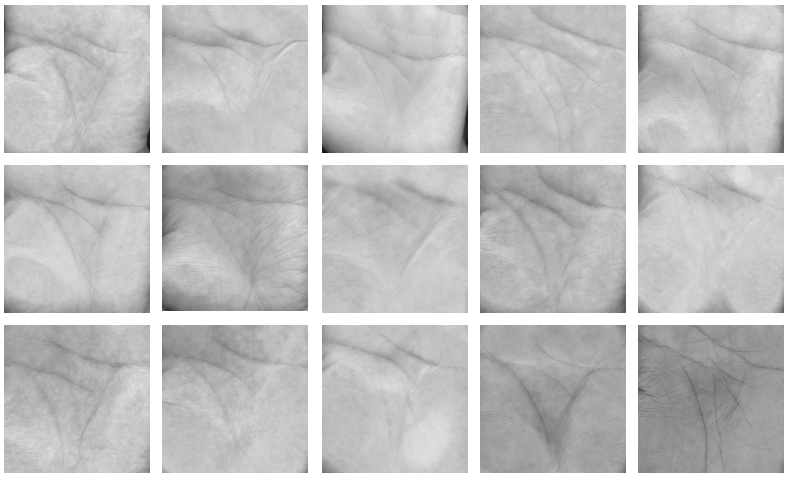

Figure 4: Training palmprints for the Left palm from each of the 15 individuals.

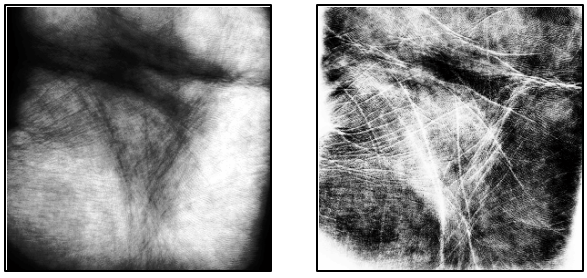

(a) (b)

Figure 5: A typical palmprint image before (a) and after normalization (b)

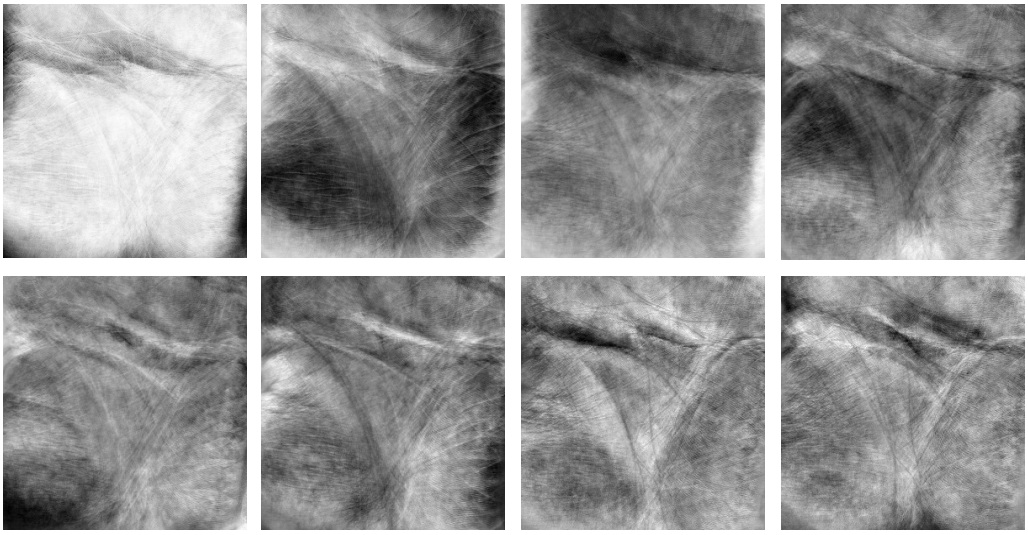

Figure 6: First eight *Eigenpalms* from the palmprints shown in figure 4.

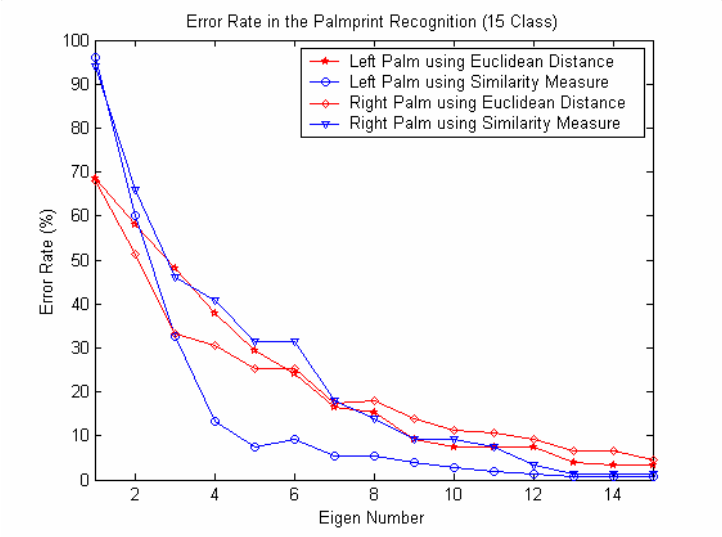

Figure 7: Error rate in the palmprint recognition for 15 class.

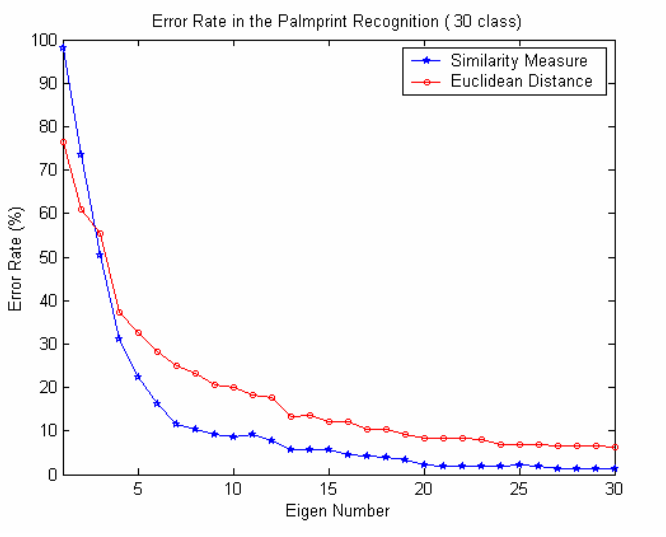

Figure 8: Error rate in the palmprint recognition for 30 class.